

Optimization of zinc sulfide thin film coating process using response surface methodology

Ersin Yücel · Yasin Yücel

Received: 5 August 2014 / Accepted: 8 October 2014 / Published online: 12 October 2014
© Springer Science+Business Media New York 2014

Abstract Zinc sulfide (ZnS) thin films have been deposited on glass substrates at room temperature using chemical bath deposition method. Application of response surface methodology and central composite design for optimizing the ZnS films deposition parameters and understanding the significance and interaction of the factors affecting the film quality was discussed in this work. pH, stirring speed and deposition time were investigated as variables and band gap was selected as response in this study. The samples were characterized using X-Ray diffraction, scanning electron microscope and ultraviolet–visible spectroscopy measurements. The optimal conditions for the deposition parameters of the ZnS thin films have been found to be: pH of 10.1, stirring speed of 163 rpm and deposition time of 31 h. Under these conditions, the experimental band gap of ZnS was 3.95 eV, which is well in close agreement with value (3.97 eV) predicted by the model.

1 Introduction

Zinc sulfide (ZnS) is a wide-band-gap semiconductor with a range of potential applications in optoelectronic devices. This semiconductor material has been studied extensively for a variety of applications, for example, in optical switching device, solar cells, photo catalysts, optical sensors, infrared windows [1–3], photo conductors, field effect

transistors, optical sensors, electroluminescent materials and phosphors materials [4].

ZnS thin films have been prepared by various techniques including solvothermal [5], spray pyrolysis [6], magnetron sputtering [7], thermal evaporation [8], photochemical deposition (PCD) [9], sol–gel [10], successive ionic layer adsorption and reaction (SILAR) [11] and chemical bath deposition (CBD) [12].

Among these methods, CBD is the most attractive approach due to a number of advantages, such as low cost, low deposition temperature, easy coating of large surfaces and can easily be applied to an industrial scale [13]. CBD process uses a controlled chemical reaction to achieve thin film deposition by precipitation. In this technique, thin films are deposited on substrates immersed in dilute solutions containing metal and chalcogenide ion sources.

The band gap is affected by many factors, such as pH, stirring speed and deposition time. The factors can be optimized by conventional one-factor-at-a-time method and statistical methods. Conventional methods involve changing one independent variable at a time, while keeping other factors at a fixed level. The response surface methodology (RSM) is a powerful technique for testing multiple process variables because fewer experimental trials are needed compared to the study of one-factor-at-a-time. Also, interactions between variables can be identified and quantified by such a technique. The method was introduced by Box–Wilson, Box–Hunter, Bradley, Davies and Hunter [14]. The main idea of RSM is to use a sequence of designed experiments to obtain an optimal response. RSM not only allows designing experiments, building models, but also used to determine optimum conditions and to evaluate the different variables [15–19]. Optimization with RSM enables the evaluation of large experimental area and it also describes the role of every variable. Also, central

E. Yücel (✉)
Department of Physics, Faculty of Arts and Sciences, Mustafa Kemal University, 31034 Antakya, Hatay, Turkey
e-mail: dr.ersinyucel@gmail.com

Y. Yücel
Department of Chemistry, Faculty of Arts and Sciences, Mustafa Kemal University, 31034 Antakya, Hatay, Turkey

composite design (CCD) is an experimental design which is useful in RSM for building a second order model for the response variable without needing to use a complete three-level factorial experiment [15].

In recent years, the applications of experimental design methodologies on semiconducting materials such as thin film studies have been increased. For example, RSM was used to optimization and modeling of preparation conditions of TiO₂ nanoparticles coated on hollow glass microspheres by Sun et al. [20]. Saikaew et al. [21] studied the optimization of carbon doped molybdenum oxide thin film coating process using designed experiments. The optimization of process parameters of titanium dioxide films worked using RSM by Tien and Lin [22]. Also, we have successfully used RSM to optimize of deposition conditions of CdS thin films prepared on glass substrates by CBD technique in our previous study [23]. It is important to investigate variations of the ZnS thin film band gap as a function of pH, stirring speed and deposition time. So far, No one has reported research on using RSM to optimize various influencing factors and their interactions during the deposition process of ZnS thin films on the glass substrates by CBD.

In this novel research, we have systematically investigated the effect of pH, stirring speed and deposition time on the band gap values. The samples were evaluated by X-ray diffractometer, scanning electron microscope (SEM) and ultraviolet–visible spectroscopy (UV–Vis) measurements. RSM was used to optimize the conditions for the deposition parameters of the samples and to understand the significance and interaction of the factors affecting the ZnS thin film band gap values.

2 Experimental procedure

ZnS thin films were fabricated by the CBD method on glass substrates. The chemicals used for the deposition were an analytical grade and purchased from Sigma-Aldrich. The solutions were prepared in deionized water and films were deposited on 75 mm × 25 mm × 1 mm commercial glass substrates. Before deposition, the substrates were rinsed in a dilute sulphuric acid solution (H₂SO₄/H₂O, 1:5, v/v) to remove native oxide layer and then completely rinsed in acetone and double distilled water for 5 min. and finally dried in air. The reaction bath solution was prepared using a mixture of 2.5 ml of 1 M ZnSO₄·7H₂O, 3 ml of 3.75 M triethanolamine [(HOCH₂CH₂)₃N], 2 ml of ammonia/ammoniumchloride (NH₃/NH₄Cl, pH:10.55), 0.1 ml of 0.66 M tri-sodiumcitrate (C₆H₅Na₃O₇), 1 ml of 1 M thi-oacetamide (CH₃CSNH₂) and 41.5 ml of deionized water. The deposition was made on the glass substrates at room temperature. The pH values of the chemical baths were determined using a pH meter (HACH sension 1). The clean

Table 1 Independent variables and levels used for response surface design

Independent variables	Symbols	Levels				
		–	–1	0	1	1.682
pH	X ₁	10.00	10.2	10.5	10.8	11.00
Stirring speed (rpm)	X ₂	116	150	200	250	284
Deposition time (h)	X ₃	28	36	48	60	68

substrates were placed vertically in the solution at the desired pH, stirring speed and deposition time without heating. After deposition, the coated substrates were taken out of the bath, rinsed with deionized water, dried in air at room temperature and preserved in an airtight plastic container. The deposited ZnS thin films were found to be uniform and well adherent to the substrates and further used for different characterizations. Then, the films were annealed in vacuum for 1 h at 500 °C .

Surface morphologies of the samples were observed using an A JEOL JSM-500LM SEM. Structural analysis were carried out by using Bruker AXS D8 Advance Model X-ray diffractometer with Cu Kα radiation (λ = 1.540056 Å) in the range 2θ = 2°–80° with a scan speed of 3°/min and a step increment of 0.02° at room temperature. Optical absorption spectra in the UV–Vis spectral range (190–1,100 nm) of the structures were determined by using a UV–Vis spectrophotometer (Thermo Scientific Genesys 10S).

3 Experimental design

Response surface methodology was used to investigate the influence of pH, stirring speed and deposition time on the ZnS thin film band gap values and the film quality. A five-level-three-factor CCD model was used to optimize of the factors. The factors and their levels were selected based on the significance of experiments. The coded and suitable uncoded values were given in Table 1. Formed CCD was illustrated in Table 2.

3.1 Statistical analysis

The experimental data provided from CCD were examined using RSM. A polynomial Eq. (1) was used to compute the predicted response:

$$Y_{yield} = b_0 + \sum_{i=1}^4 b_i X_i + \sum_{i=1}^4 b_{ii} X_i^2 + \sum_{i < j}^4 \sum_{iZj} b_{ij} X_i X_j \quad (1)$$

where Y_i is the experimental response, b₀ is the offset term, b_i is the linear effect, b_{ii} is the squared effect, b_{ij} is the interaction

Table 2 Experimental setup for five-level, three-factor surface response design and the experimental data with coded and actual values of variables

Experiment	Coded independent variable levels			Actual values of variables			Band Gap (eV)	
	X_1	X_2	X_3	pH, X_1	Stirring speed (rpm), X_2	Deposition time (h), X_3	Experimental	Predicted
1	-1	-1	-1	10.2	150	36	3.93	3.94
2	1	-1	-1	10.8	150	36	3.65	3.67
3	-1	1	-1	10.2	250	36	3.93	3.91
4	1	1	-1	10.8	250	36	3.68	3.70
5	-1	-1	1	10.2	150	60	3.91	3.90
6	1	-1	1	10.8	150	60	3.57	3.60
7	-1	1	1	10.2	250	60	3.92	3.91
8	1	1	1	10.8	250	60	3.65	3.66
9	-1.682	0	0	10	200	48	3.93	3.95
10	1.682	0	0	11	200	48	3.56	3.52
11	0	-1.682	0	10.5	116	48	3.81	3.79
12	0	1.682	0	10.5	284	48	3.81	3.82
13	0	0	-1.682	10.5	200	28	3.88	3.86
14	0	0	1.682	10.5	200	68	3.80	3.80
15	0	0	0	10.5	200	48	3.82	3.82
16	0	0	0	10.5	200	48	3.82	3.82
17	0	0	0	10.5	200	48	3.79	3.82
18	0	0	0	10.5	200	48	3.82	3.82
19	0	0	0	10.5	200	48	3.84	3.82
20	0	0	0	10.5	200	48	3.81	3.82

effect, x_i is the i th independent variable and x_j is the j th independent variable. Design Expert 7.0.0 Software (STAT-EASE Inc., Minneapolis, USA) was used to analyse of the experimental data. F-test used to interpret the coefficients. CCD was used to optimize the ZnS thin film deposition parameters. Regression analysis was performed for each response in order to estimate the effect of combined independent variables on the responses. Each response was tested for possible linear, quadratic and cubic models to find out to best fitting model. Quadratic polynomial model was used to calculate regression coefficients. Significance of each model term was determined with analysis of variance (ANOVA). The fit of the models were evaluated by R^2 . The statistical significance was checked by F-test. Response surface plots were drawn based on the equation to demonstrate the effects of independent variables on the response.

4 Results and discussion

4.1 Optimization of deposition parameters of ZnS thin films

The deposition conditions of ZnS thin films optimized using CCD model. The predicted and experimental response of the independent variables is shown in Table 2.

Band gap values of the samples ranged from 3.56 to 3.93 eV. Interactions of factors and its effects calculated using Design Expert 7.0.0 Software (STAT-EASE Inc., Minneapolis, USA). The model described by Eq. (2) represents ZnS thin film band gap values (y) as a function of pH (x_1), stirring speed (x_2) and deposition time (x_3).

$$y = 3.817 - 0.129x_1 + 0.009x_2 - 0.020x_3 + 0.013x_1x_2 - 0.010x_1x_3 + 0.008x_2x_3 - 0.029x_1^2 - 0.006x_2^2 + 0.005x_3^2 \quad (2)$$

Equation (2) was checked by F-test and ANOVA for the second order polynomial model is given in Table 3. The model was highly significant and sufficient to represent the actual relationship between the response and significant parameters with very low p value (<0.0001) from the ANOVA. The computed model F-value (40.42) implies the model is significant. The value of R^2 was also given in Table 3. A good coefficient of determination ($R^2 = 0.9732$) obtained from the ANOVA. The coefficient of determination also demonstrated that there are perfect correlations between the independent variables. The lack of fit (F-value: 4.15) value for regression of Eq. (2) is not significant. Non-significant lack of fit is good and displays that the model equation was sufficient for predicting the

Table 3 Analysis of variance (ANOVA) for the fitted quadratic polynomial model for optimization of ZnS thin film deposition parameters

Source	Sum of squares	Degree of freedom	Mean square	F-value	<i>p</i> value (Prob > F)
Model	0.25	9	0.028	40.42	<0.0001 ^a
pH (<i>x</i> ₁)	0.23	1	0.23	331.44	<0.0001 ^a
Stirring speed (<i>x</i> ₂)	1.054E – 003	1	1.054E – 003	1.54	0.2434 ^b
Deposition time (<i>x</i> ₃)	5.519E – 003	1	5.519E – 003	8.04	0.0177 ^a
<i>x</i> ₁ <i>x</i> ₂	1.250E – 003	1	1.250E – 003	1.82	0.2068 ^b
<i>x</i> ₁ <i>x</i> ₃	8.000E – 004	1	8.000E – 004	1.17	0.3056 ^b
<i>x</i> ₂ <i>x</i> ₃	4.500E – 004	1	4.500E – 004	0.66	0.4369 ^b
<i>x</i> ₁ ²	0.012	1	0.012	17.63	0.0018 ^a
<i>x</i> ₂ ²	5.173E – 004	1	5.173E – 004	0.75	0.4056 ^b
<i>x</i> ₃ ²	3.069E – 004	1	3.069E – 004	0.45	0.5188 ^b
Residual	6.861E – 003	10	6.861E – 004		
Lack of fit	5.528E – 003	5	1.106E – 003	4.15	0.0723 ^b
Pure Error	1.333E – 003	5	2.667E – 004		
Cor total	0.26	19			
R ² = 0.9732					

^a Significant at “Prob > F” less than 0.05

^b Insignificant at “Prob > F” more than 0.05

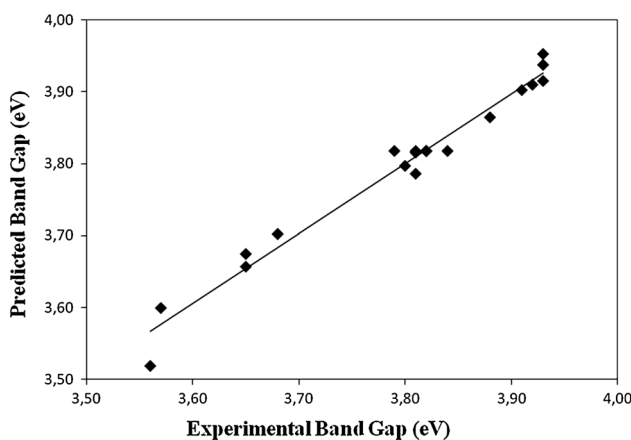


Fig. 1 Predicted ZnS thin film band gap versus experimental ZnS thin film band gap

ZnS thin film band gaps. The effects of the samples deposition parameters such as pH, stirring speed and deposition time were investigated on the film band gap values. The significance of coefficients determined with *p* values and smaller the *p* value shows the more significant the corresponding coefficient. According to Table 3 *x*₁ (pH), *x*₃ (deposition time) and *x*₁² are the most significant parameters. However, *x*₂ (stirring speed), *x*₁*x*₂, *x*₁*x*₃, *x*₂*x*₃, *x*₂² and *x*₃² have less effect on the thin film band gaps. The relationship between predicted and experimental band gap values is shown in Fig. 1. It can be seen that observed band gaps of the films (the response) agreed well (R² = 0.9732) with the predicted data.

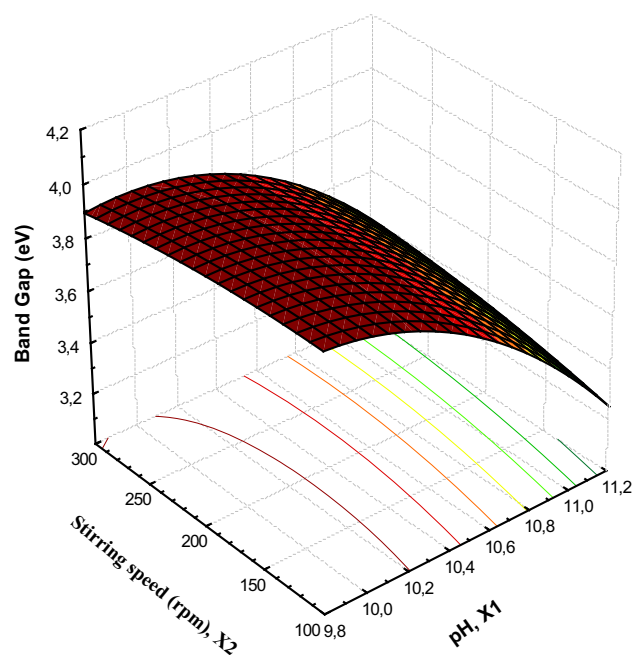


Fig. 2 Response surface plot of ZnS thin film band gap (eV) predicted from the quadratic model. The effect of pH (*X*₁), stirring speed (*X*₂) and their reciprocal interaction on the ZnS thin film band gap (eV)

The response surface plots were obtained using Statistica 8.0 Software (STATSOFT, Inc., Oklahoma, USA). Based on the developed model [Eq. (2)], the response surface plots for the interaction effects of the factors can be seen in Figs. 2, 3 and 4. Figure 2 showed the interaction relationship between the two independent variables (pH

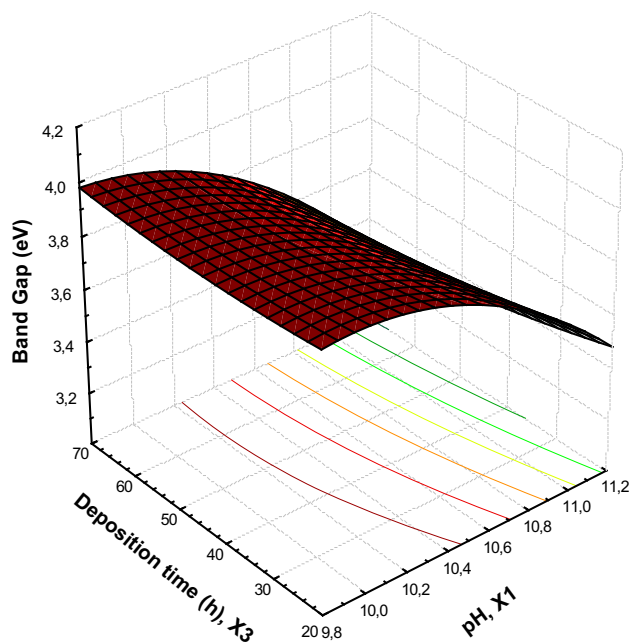


Fig. 3 Response surface plot of ZnS thin film band gap (eV) predicted from the quadratic model. The effect of pH (X_1), deposition time (X_3) and their reciprocal interaction on the ZnS thin film band gap (eV)

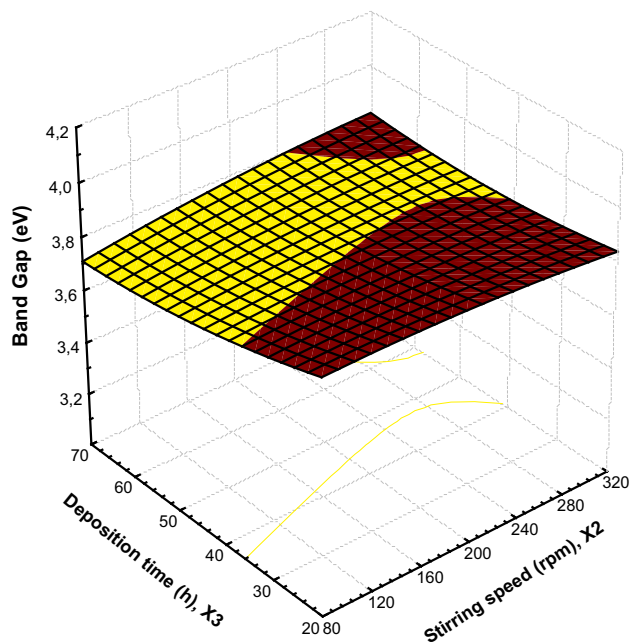


Fig. 4 Response surface plot of ZnS thin film band gap (eV) predicted from the quadratic model. The effect of stirring speed (X_2), deposition time (X_3) and their reciprocal interaction on the ZnS thin film band gap (eV)

and stirring speed) and their effects on the response variable (the band gaps of the samples). It was indicated that the thin film band gap values reduced with increasing of

pH. Similar trend was observed by Kang et al. [24]. But increasing of stirring speed was not observed any important differences on the band gap values. The same pattern was reported by Zhang et al. [25].

The effect of pH and deposition time and their opposed interaction on the ZnS band gap is illustrated in Fig. 3. According to the figure, the ZnS thin film band gap value reduced with increasing of pH similarly at Fig. 2 whereas increasing of deposition time was observed a little difference on the band gap especially at high pH values. The band gap a little reduced with increasing of deposition time at high pH values. Similar behaviours have been reported by Agawane et al. [26].

Figure 4 represents the effects of varying stirring speed and deposition time on the ZnS thin film band gaps. Increasing of stirring speed was not observed to cause any important differences on the band gap values. The result was in accordance with reported in literature [25]. Also this result was in accordance with reported in Fig. 2. Whereas the band gap a little reduced with increasing of deposition time at different stirring speed values. Similar trend was observed by Agawane et al. [26].

The composition of optimum ZnS thin film band gap value was identified from the Eq. 2. Optimum conditions for the deposition parameters of the films were determined to be 10.1 (pH), 163 rpm (stirring speed) and 31 h (deposition time). The model accuracy verified by working under optimum conditions. Experimental thin film band gap was found as 3.95 eV. Also predicted band gap value was calculated as 3.97 eV from the model. Results indicated that validity of the predicted model confirmed by verification experiments. According to results, the model was considered to be correct and reliable for predicting the ZnS thin film band gap value for deposition of the samples using CBD method.

4.2 Structural and morphological properties

The morphologies and microstructures of the ZnS thin film samples were examined by scanning electron microscopy. Figure 5 shows the SEM image of the sample fabricated under the optimum deposition conditions (pH = 10.1, stirring speed = 163 rpm and deposition time = 31 h). As shown in Fig. 5, the obtained film consisted of densely packed spherical grains. It can also be seen that from the figure the film is uniform, smooth, homogeneous, and continuous and the substrate was well covered by ZnS particles.

Generally, ZnS exists in sphalerite, cubic, zinc blende type structure or hexagonal, wurtzite type structure depending on deposition conditions. The cubic type structure is stable at room temperature, while hexagonal type structure is at high temperature [24, 27]. X-Ray

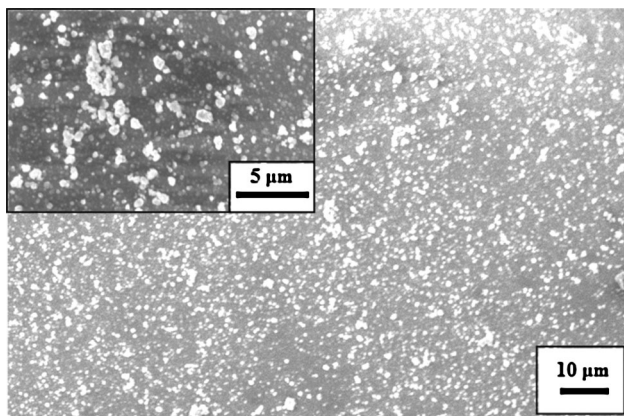
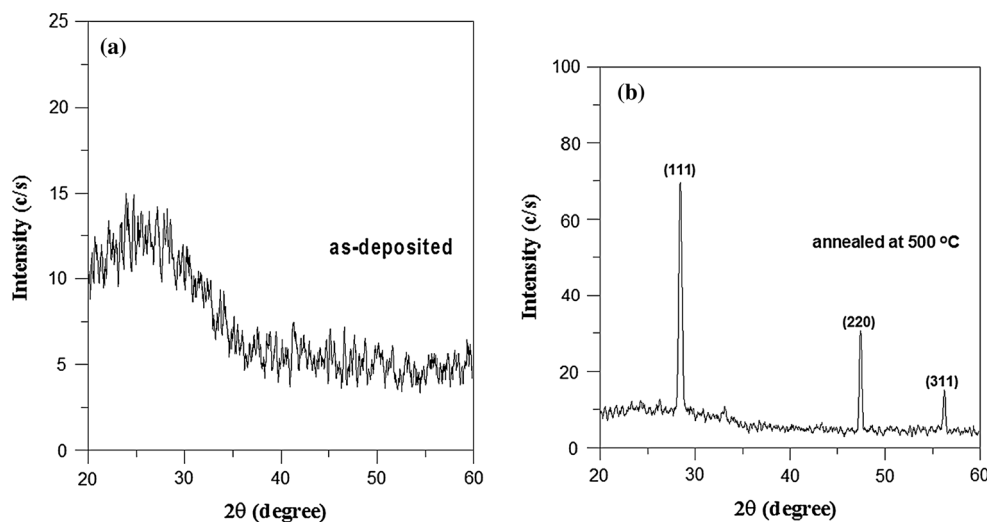


Fig. 5 SEM micrographs of ZnS thin film grown under the optimum fabrication conditions

diffraction (XRD) analyses were employed to study the crystal structures of the films. The XRD patterns for as-deposited and annealed (500 °C) of the sample fabricated under the optimum deposition conditions (pH = 10.1, stirring speed = 163 rpm and deposition time = 31 h), are shown in Fig. 6. Figure 6a shows that while before annealing the film is amorphous and the broad hump between 20° and 35° is due to the amorphous glass substrate. As can be seen from the Fig. 6b that three reflection peaks are observed in the orientations of (111), which is most intensive, (220) and (311) at $2\theta = 28.50^\circ, 47.50^\circ$ and 57.80° respectively. These values are in agreement with standard data of Joint Committee on Powder Diffraction Standards (JCPDS) data [28]. No characteristic peaks of impurity phases such as ZnO or Zn(OH)₂ were detected. It can be concluded that the ZnS thin film grown by CBD method in this study has the cubic structure.

Fig. 6 X-ray diffraction pattern of ZnS thin film grown under the optimum fabrication conditions: **a** as-deposited at room temperature **b** annealed at 500 °C



The crystallite sizes of the ZnS thin films were calculated from Debye–Scherrer equation [16]

$$D = k\lambda/\beta \cos \theta \tag{3}$$

where, D = average crystallite size, λ = wavelength of X-ray radiation, β = full width of half maximum intensity (FWHM) of the XRD spectrum of ZnS thin films, θ = Bragg angle and k = Scherrer constant. Here k is 0.94.

The average crystalline sizes of the films were calculated by resolving the highest intense peaks of ZnS films within the range 30 nm to 0.4 μm with different deposition conditions.

4.3 Optical properties

Optical absorption spectra in the UV–Vis spectral range (190–1,100 nm) of the ZnS thin film samples were determined using a UV–Vis spectrophotometer. Analysis of the dependence of absorption coefficient on photon energy in the high absorption regions was performed to obtain information on the energy band gaps of the ZnS thin films. The optical band gap values were determined by the following relation [29].

$$(\alpha h\nu) = C(h\nu - E_g)^{n/2} \tag{4}$$

where C is an energy-independent constant, E_g is the optical band gap and n is an index that characterizes the optical absorption process; n is theoretically equal to 1 and 4 for direct band gap semiconductor and indirect band gap semiconductor materials, respectively. According to theoretical and experimental results, ZnS exhibits direct transitions between valance and conduction bands [30]. Thus n can be chosen as 1. Plotting the graph of $(\alpha h\nu)^2$ against

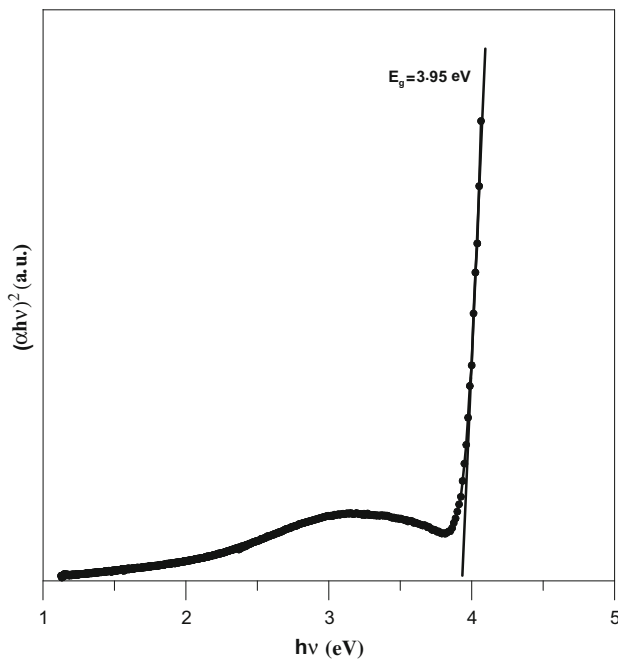


Fig. 7 Plot of $(\alpha hv)^2$ versus $h\nu$ for ZnS thin film grown under the optimum fabrication conditions

photon energy ($h\nu$), the band gap (E_g) value can be determined by extrapolating the straight-line portion.

Figure 7 illustrates plots of $(\alpha hv)^2$ versus $h\nu$ for the sample fabricated under the optimum deposition conditions (pH = 10.1, stirring speed = 163 rpm and deposition time = 31 h). The E_g values of the samples were found in between 3.56 and 3.93 eV. As the pH value decreases from 11 to 10, the band gap of the samples increases from 3.56 to 3.93 eV. We think that this increase can be explained on the basis of quantum size effect. The particle size of the ZnS thin film decrease with increasing the band gap; this is known as the quantum size effect. Quantum size effect could be substantially different depending on the deposition conditions and kind of precursor materials [31]. Furthermore, pH plays a significant role in the structural properties of the ZnS films. Influence of the pH on the optical band gap of ZnS films shows in Figs. 2 and 3. As can be seen from these figures, the E_g of the ZnS film decreased with increasing pH value of the solution from 10 to 11. The decrease in E_g with increase in pH can be explained in terms of structural changes occurring in the thin film. Changes in pH are mainly caused the change of the structural and morphological features such as the crystallinity degree and the porosity. Additionally, similar behaviours have been reported by Yücel et al. [23], Preetha et al. [32], Remadevi et al. [33] and Addonizio et al. [34]. As the deposition time increases from 28 h to 68 h, the band gap of the samples decreases from 3.88 to 3.80 eV. This decrease could be attributed to quantum size effect

due to the small grain sizes of the ZnS films. Because the average particle sizes of the samples increased with increasing of deposition times. Increasing of stirring speed was not observed to cause any important differences on the ZnS thin film band gap values.

5 Conclusions

In this study, ZnS thin films were successfully deposited on glass substrates at room temperature by CBD method. For the first time, RSM and CCD have been used to optimize the samples deposition parameters and to understand the significance and interaction of the factors affecting the film quality. A quadratic polynomial model was provided to explain the relationship between the band gap value and the parameters of pH, stirring speed and deposition time. The results indicated that pH and deposition time were the significant factors on the band gap. The optimum conditions for the deposition parameters of the ZnS thin films were pH of 10.1, stirring speed of 163 rpm and deposition time of 31 h. The experimental E_g value of the film (3.95 eV) agreed with the predicted value (3.97 eV) within a good confidence level, thus indicating the suitability of RSM in optimising the conditions for the deposition parameters of the films.

The wide band gap of these films makes it possible to use them as buffer layer for solar cells.

References

1. S.M. Pawar, B.S. Pawar, J.H. Kim, O.S. Joo, C.D. Lokhande, *Curr. Appl. Phys.* **11**, 117–161 (2011)
2. J. Kessler, J. Wennerberg, M. Bodegard, L. Stolt, *Sol. Energ. Mat. Sol. C.* **75**, 35–46 (2003)
3. M. Stefan, E.J. Popovici, O. Pana, E. Indrea, *J. Alloys Compd.* **548**, 166–172 (2013)
4. S. Takata, T. Minami, T. Miyata, *Thin Solid Films* **193–194**, 481–488 (1990)
5. Y. Li, Y. Liu, W. Shen, Y. Yang, Y. Wen, M. Wang, *Mater. Lett.* **65**, 2518–2521 (2011)
6. J.W. Li, Y.K. Su, M. Yokoyam, *Jpn. J. Appl. Phys.* **33**, 4723–4726 (1994)
7. X.J. Zheng, Y.Q. Chen, T. Zhang, B. Yang, C.B. Jiang, B. Yuan, Z. Zhu, *Sens. Actuators B* **147**, 442–446 (2010)
8. V. Dimitrova, J. Tate, *Thin Solid Films* **365**, 134–138 (2000)
9. F. Goto, M. Ichimura, E. Arai, *Jpn. J. Appl. Phys.* **36**, 1146–1149 (1997)
10. Y. Kavanagh, M.J. Alam, D.C. Cameron, *Thin Solid Films* **447–448**, 85–89 (2004)
11. Y.F. Nicolau, *Appl. Surf. Sci.* **22–3**, 1061–1074 (1985)
12. L. Zhou, N. Tang, S. Wu, *Surf. Coat. Technol.* **228**, S146–S149 (2013)
13. J. Cheng, D.B. Fan, H. Wang, B.W. Liu, Y.C. Zhang, H. Yan, *Semicond. Sci. Technol.* **18**, 676 (2003)

14. J.A. Cornell, How to Apply Response Surface Methodology (US: Am Soc Qual Control: Statistic Division; 1990)
15. R.G. Brereton, *Chemometrics: Data Analysis For The Laboratory and Chemical Plant* (Wiley, London, 2003)
16. E. Yücel, Y. Yücel, İ. Belenli, *J. Mater. Sci.: Mater. Electron.* **23**, 1284–1292 (2012)
17. Y. Yücel, *Fuel Process. Technol.* **99**, 97–102 (2012)
18. Y. Yücel, *Biocatal. Agric Biotechnol.* **1**, 39–44 (2012)
19. K. Ali, S.A. Khan, M.Z.M. Jafri, *Superlattices Microstruct.* **52**, 782–792 (2012)
20. L. Sun, S. Wanb, Z. Yu, L. Wang, *Sep. Purif. Technol.* **125**, 156–162 (2014)
21. C. Saikaew, A. Wisitsoraat, R. Sootticoon, *Surf. Coat. Technol.* **204**, 1493–1502 (2010)
22. C.L. Tien, S.W. Lin, *Opt Commun* **266**, 574–581 (2006)
23. E. Yücel, N. Güler, Y. Yücel, *J. Alloys Compd.* **589**, 207–212 (2014)
24. S.R. Kang, S.W. Shin, D.S. Choi, A.V. Moholkar, J.H. Moon, J.H. Kim, *Curr. Appl. Phys.* **10**, S473–S477 (2010)
25. Y. Zhang, X.Y. Dang, J. Jin, T. Yu, B.Z. Li, Q. He, F.Y. Li, Y. Sun, *Appl. Surf. Sci.* **256**, 6871–6875 (2010)
26. G.L. Agawane, S.W. Shin, M.S. Kim, M.P. Suryawanshi, K.V. Gurav, A.V. Moholkar, J.Y. Lee, J.H. Yun, P.S. Patil, J.H. Kim, *Curr. Appl. Phys.* **13**, 850–856 (2013)
27. Z.Q. Li, J.H. Shi, Q.Q. Liu, Z.A. Wang, Z. Sun, S.M. Huang, *Appl. Surf. Sci.* **257**, 122–126 (2010)
28. JCPDS Powder Diffraction File, card no: 05-0566; 1999
29. S. Kahraman, H.M. Çakmak, S. Çetinkaya, F. Bayansal, H.A. Çetinkara, H.S. Güder, *J. Cryst. Growth* **363**, 86–92 (2013)
30. S.W. Shin, G.L. Agawane, M.G. Gang, A.V. Moholkar, J.H. Moon, J.H. Kim, J.Y. Lee, *J. Alloys Compd.* **526**, 25–30 (2012)
31. J. Lee, S. Lee, S. Cho, S. Kim, I.Y. Park, Y.D. Choi, *Mater. Chem. Phys.* **77**, 254–260 (2003)
32. K.C. Preetha, K.V. Murali, A.J. Ragina, K. Deepa, T.L. Remadevi, *Curr. Appl. Phys.* **12**, 53–59 (2012)
33. T.L. Remadevi, K.C. Preetha, *J. Mater. Sci.: Mater. Electron.* **23**, 2017–2023 (2012)
34. M.L. Addonizio, A. Aronne, S. Daliento, O. Tari, E. Fanelli, P. Pernice, *Appl. Surf. Sci.* **305**, 194–202 (2014)